CORA Cork Open Research Archive
Cartlann Taighde Oscailte Chorcaí

Title	AuxAg1-x alloy seeds: A way to control growth, morphology and defect formation in Ge nanowires
Authors	Biswas, Subhajit;Holmes, Justin D.
Publication date	2012-06-01
Original Citation	Biswas, S. and Holmes, J. D. (2012) 'AuxAg1-x alloy seeds: A way to control growth, morphology and defect formation in Ge nanowires' . Nanotech 2012. 18-21 June. Santa Clara, CA. In: Nanotech 2012, Vol. 1. pp. 749-752. ISBN: 978-1-4665-6274-5
Type of publication	Conference item
Link to publisher's version	http://www.nsti.org/procs/Nanotech2012v1/1/W2.112
Rights	© 2012 Nano Science and Technology Institute.
Download date	2026-10-17 10:06:47
Item downloaded from	https://hdl.handle.net/10468/2598

UCC
University College Cork, Ireland
Coláiste na hOllscoile Corcaigh

Au_xAg_{1-x} alloy seeds: A way to control growth, morphology and defect formation in Ge nanowires

Subhajit Biswas[*] and Justin D Holmes[*,**]

[*]Materials Chemistry & Analysis Group, Department of Chemistry and the Tyndall National Institute, University College Cork, Cork, Ireland

[**] Centre for Research on Adaptive Nanostructures and Nanodevices, Trinity College Dublin, Dublin 2, Ireland

ABSTRACT

Germanium (Ge) nanowires are of current research interest for high speed nanoelectronic devices due to the lower band gap and high carrier mobility compatible with high K-dielectrics and larger excitonic Bohr radius ensuing a more pronounced quantum confinement effect [1-6]. A general way for the growth of Ge nanowires is to use liquid or a solid growth promoters in a bottom-up approach which allow control of the aspect ratio, diameter, and structure of 1D crystals via external parameters, such as precursor feedstock, temperature, operating pressure, precursor flow rate etc [3, 7-11]. The Solid-phase seeding is preferred for more control processing of the nanomaterials and potential suppression of the unintentional incorporation of high dopant concentrations in semiconductor nanowires and unrequired compositional tailing of the seed-nanowire interface [2, 5, 9, 12]. There are therefore distinct features of the solid phase seeding mechanism that potentially offer opportunities for the controlled processing of nanomaterials with new physical properties. A superior control over the growth kinetics of nanowires could be achieved by controlling the inherent growth constraints instead of external parameters which always account for instrumental inaccuracy. The high dopant concentrations in semiconductor nanowires can result from unintentional incorporation of atoms from the metal seed material, as described for the Al catalyzed VLS growth of Si nanowires [13] which can in turn be depressed by solid-phase seeding. In addition, the creation of very sharp interfaces between group IV semiconductor segments has been achieved by solid seeds [14], whereas the traditionally used liquid Au particles often leads to compositional tailing of the interface [15] . Korgel *et al.* also described the superior size retention of metal seeds in a SFSS nanowire growth process, when compared to a SFLS process using Au colloids [12].

Here in this work we have used silver and alloy seed particle with different compositions to manipulate the growth of nanowires in sub-eutectic regime. The solid seeding approach also gives an opportunity to influence the crystallinity of the nanowires independent of the substrate. Taking advantage of the readily formation of stacking faults in metal nanoparticles, lamellar twins in nanowires could be formed.

keywords: alloy nanoparticles, nanowires, germanium, transmission electron microscopy, twin boundary.

1 EXPERIMENTAL

Ge nanowires were grown in a stainless steel cell (High Pressure Equipment Company) at temperatures between 370-450 ºC. In a typical experiment the nanoparticle colloids were deposited on a (001) silicon substrate and loaded in a stainless steel cell and dried under vacuum at 180 ºC for 48h. 4 ml toluene was filled in the 5 ml reaction cell and the assembly heated to 390-400 ºC in a tube furnace. After setting the pressure to exactly 21 MPa, the injection cell, filled with 20 ml of toluene/diphenylgermane solution, was set to the identical pressure. The precursor solution was injected in a rate of 1.5-2 ml/h over a time period of 30-240 min at constant pressure conditions. Finally reaction cell was cooled to room temperature, depressurized and disassembled to access the growth substrate.

Characterization

The deposits of 1D Ge nanostructures were analysed using a FEI quanta 650 scanning electron microscope (SEM) and a Jeol 2100 transmission electron microscope (TEM) operated at 200 kV equipped with an EDX detector.

2 RESULTS & DISCUSSION

4 nm dodecanethiol stabilized Ag and alloy nanoparticles (NPs) were synthesized by co-reducing the mixture of chlorauric acid (HAuCl4) and silver nitrate (AgNO3) in the chloroform/water biphasic solution [16]. Ag nanocrystals, with a nominal diameter of 6.3 (±0.5) nm were synthesized by the thermal decomposition of silver acetate in a high boiling point solvent [17] . The NPs were precipitated with ethanol and redispersed in toluene for further use. Figure 1a shows the TEM image of representative 4 nm diameter alloy NPs. Figure 1b shows the UV-vis spectra of the as-synthesized NPs where a single surface plasmon resonance (SPR) peak can be observed. The SPR peak red shifts with the addition of more Au component in the alloy, suggeting the formation of AgAu alloy NP. A supercritical-fluid-solid-solid (SFSS) approach

was adopted for the growth of nanowires onto (001) silicon substrate in a supercritical toluene medium using the thermolysis of diphynyelgermane. As expected from the theoritical assumption, effective growth of Ge nanowires was achieved for Ag and different alloy nanoparticles. Representative SEM images shown in figure 2a and b depict nanowires with high aspect ratio for Ag and alloy NP seeds. The diameter of the nanowires lies within 10-40 nm whereas the length is in the order of micrometers. Inset of figure 2a shows a TEM image.

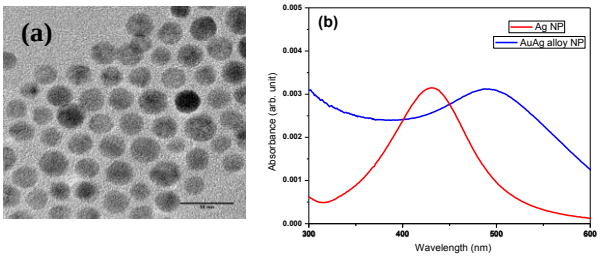

Figure 1: Representative TEM image of (a) alloy nanoaprticles of 4 nm diameter. (b) Optical absorbance spectra of the nanoparticles.

Rrepresentative TEM and high resolution TEM images (Fig. 2c and d) and corresponding fast Fourrier transformation (FFT) pattern (in the inset) exhibit very thin amophous shell and formation of bulk diamond cubic crystal structure (PDF 04-0545) with nanowire growth directions along [111] which is the most commonly reported growth axis for Ge nanowires.

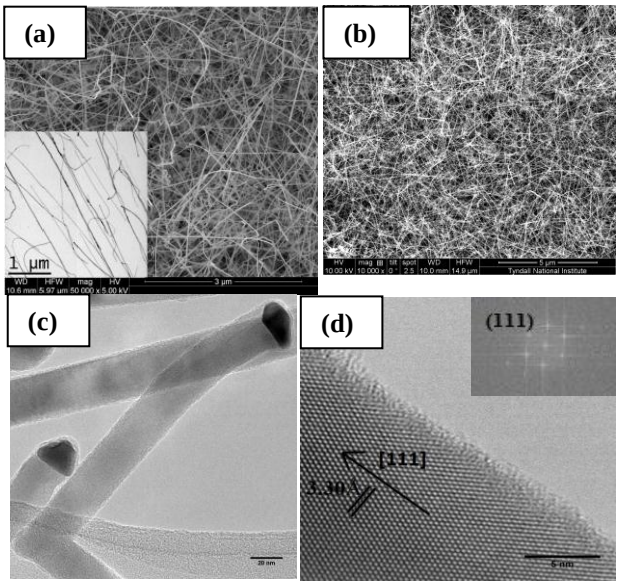

Figure 2: Representative SEM images of Ge nanowires grown with (a) 6 nm Ag and (b) 4 nm alloy nanopartice. (c) TEM image shows no amorphous shell (d) HRTEM image depicting [111] growth direction of a nanowire.

Electron diffraction spectroscopy (EDS) measurement (Fig. 3) from the metal tip and body of the nanowire confirms the presence of both Ag and Au for the tip and Ge in the length of the nanowire. After 45 mins of growth using the similar experimental parameters for all the different NP seeds, a difference in the lengthe and diameter in nanowires was observed from the SEM. It appears that the diameter varies from 30-40 nm to 12-15nm for Ag and alloy seeds respectively.

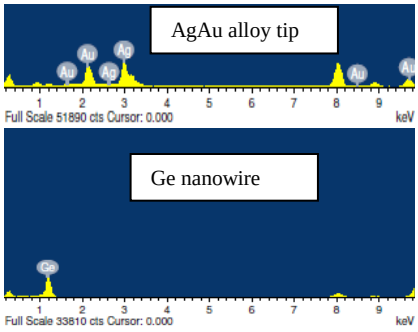

Figure 3: EDS spectra taken from alloy metal tip and nanowire body indicating presence of both Ag and Au at tip and Ge in body.

The diameter of the nanowires are much thinner (~12-15 nm) for alloy seeding. The slower coalescence kinetics of alloy NPs is responsible for much thinner nanowires with narrow diameter distribution. Lower tendency of coalesce due to their higher melting point (compared to Ag) and faster diffusion kinetics of Ge in make alloy NPs a suitable candidate to promote the growth of long and very thin nanowires. It was reported that the time for sintering of two equal size spheres in contact is $\infty r^4T/B$ [18], where r and T is the particle radius and temperature respectively and B is a constant which is proportional to surface energy and diffusivity. The Boltzmann-Arrhenius dependency of diffusivity with temperature follows $D= D_o\exp(-E_a/RT)$, where D_o pre-exponential diffusion coefficient, E_a is the activation energy which is proportional to T_m (melting point in bulk) and R is the universal gas constant. Since the surface energy contribution for these metals is sufficiently small, the faster coalescence for pure Ag can be attributed to the rapid self mobility of Ag atoms due to much lowered melting point compared to the alloys producing narrow diameter distribution. With decreasing concentration of NPs (1:10 and 1:30 dilution of original solution) much thinner nanowire growth was achieved (Fig. 4a). Diameter distribution measurements from TEM (Fig. 4b and c) depicted the radial dimension in the order of 6 (± 2.43) nm and 10.1 (±3.2) nm for lower and higher concentration respectively. Higher concentration (1:10) of NPs are preferable for the relatively higher yield of nanowires. Lower synthesis temperature and low concentraion of germanium precursor ensure no or minimum side wall attachment of Ge species and hence thinner redial dimension. Higher temperature was also avoided to prevent

the formation of amorphous shells surrounding the nanowires and the secondary nucleation of particles due to the kinetically enhanced thermal decomposition of the diphenylgermane precursor at elevated temperatures.

Taking advantage of epitaxial information transfer from solid seed particles to nanowires it is possible to

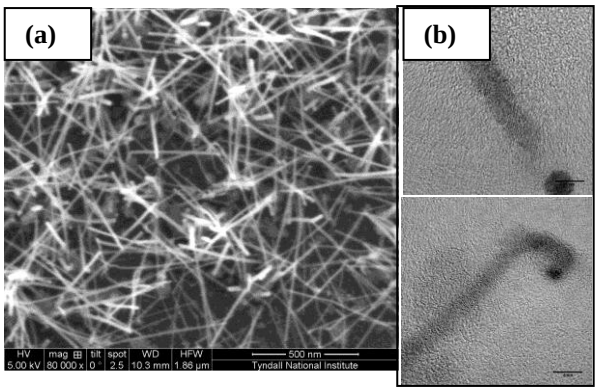

Figure 4: Representative (a) SEM and (b) HRTEM images super-thin nanowires grown with alloy seeds.

encourage unprecedented amount of planar defect formation in nanowires. Metal seeds can act as preferred growth promoter for defcet transformation if they obey the prerequisite of (a) having low twin formation energy (b) remaining in solid state during nanowires growth (c) no change in phase with Ge intake for the defect transformation process. Silver seed could serve as a perfect growth initiator as they abide the preconditions for defect induction in nanowires. Au[19] or Ni [2, 12] seeding generally produce less than 5% [112] directed twinned nanowires as the contact angle fluctuation cannot support the accommodation of sidewall faceting of a twinned plane [19]. As expected from theoretical assumption, 6 nm Ag seed encourages the growth of large number of axially twinned nanowires in the samples. The regular appearance of twin planes in the Ag seed particles and the corresponding Ge nanowires grown from them is shown in figure 5a and b. The images depict the interaction of the defects in seed particles and the Ge nanowires from their identical brightness contrast pattern. This is due to the diffraction from different crystallite segments due to their orientation to the impinging electron beam. High resolution TEM images figure 5c and d clearly illustrate the formation of {111} twin planes with [112] growth axis. Invariable formation of twin boundaries on low indices planes is associated with the low surface energy at the interface between twin and parent crystal. The creation of a defect site in the semiconductor can be observed at these kink sites at the interface. The steps are a side effect of the defects in the seed crystal, due to the energetically favored arrangement of atoms at the metal particle grain boundary [20], and result in a progression of this imperfection beyond the particle-wire interface into the Ge lattice. In addition, the defect sites in the seed particles could allow a preferential diffusion path for Ge atoms to be incorporated at the interface, as observed in the enhanced chemical diffusion along the interfaces in bicrystals [21] and along the {111} surfaces in fcc Cu when compared to other crystal directions [22]. Another explanation for the effective defect transfer, given the rough/slanted nanoparticle interface, would include a layer by layer growth of (111) layers underneath the metal particle, where the edges provide nucleation sites for the simultaneous growth of Ge layers on each subsection of the twinned semiconductor-metal particle interface [23]. The particle to nanowire interface is generally very dynamic, constantly fluctuating, forming and annihilating facets as seen in dynamic TEM studies for the solid-phase seeding of Si nanowires via palladium-silicide particles [24]. The wetting of non-planar or stepped surfaces always favors the attachment of diffusing species on step edges or surface defects. Given an uneven Ge-Ag interface, the arrangement continuously provides nucleation sites at the interface, which might be comparable to the screw-dislocation driven growth of 1D nanostructures [25].

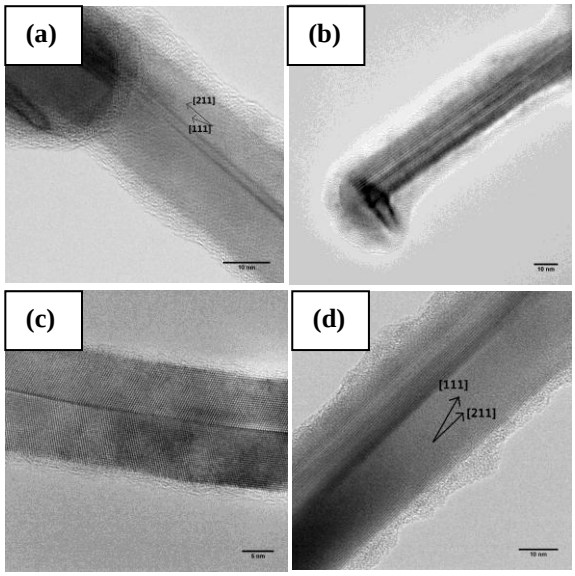

Figure 5: TEM images in part a and b showing defect transfer from metal tips to nanowires from their identical brightness-contrast patterns. HRTEM images in (c) and (d) illustrate the formation of {111} twin planes with [112] being the nanowires growth axis.

In summary, we have demonstrated the use of Ag and alloy seeds to grow 1-D germenium crystals. With increased popularity of solid phase seeding these new seed materials could be appealing for nanowire growth for other materials also. This nanoparticles seeds can produce thin and long nanowires. We have also shown that silver seeds are capable to induce twinning boundary in a large number

of growing nanowires. A high percentage of nanowires with {111} twinning defects were observed for silver seeded growth. These investigations and concept allow the future formation of defined twinning events in nanowires.

REFERENCES

[1] J. Andzane, N. Petkov, A. I. Livshits, J. J. Boland, J. D. Holmes,D. Erts; Nano Lett., 2009, 9, 1824.
[2] S. Barth, M. M. Kolesnik, K. Donegan, V. Krstic,J. D. Holmes; Chem. Mat., 2011, 23, 3335.
[3] G. Collins, M. Kolesnik, V. Krstic,J. D. Holmes; Chem. Mat., 2010, 22, 5235.
[4] S. A. Dayeh,S. T. Picraux; Nano Lett., 2010, 10, 4032.
[5] H. Geaney, C. Dickinson, C. A. Barrett,K. M. Ryan; Chem. Mat., 2011, 23, 4838.
[6] T. Hanrath,B. A. Korgel; Advanced Materials, 2003, 15, 437.
[7] S. Kodambaka, J. Tersoff, M. C. Reuter,F. M. Ross; Science, 2007, 316, 729.
[8] M. Koto, A. F. Marshall, I. A. Goldthorpe,P. C. McIntyre; Small, 2010, 6, 1032.
[9] J. L. Lensch-Falk, E. R. Hemesath, D. E. Perea,L. J. Lauhon; J. Mater. Chem., 2009, 19, 849.
[10] M. Simanullang, K. Usami, T. Kodera, K. Uchida,S. Oda; Jpn. J. Appl. Phys., 2011, 50.
[11] X. Y. Wu, J. S. Kulkarni, G. Collins, N. Petkov, D. Almecija, J. J. Boland, D. Erts,J. D. Holmes; Chem. Mat., 2008, 20, 5954.
[12] H. Y. Tuan, D. C. Lee, T. Hanrath,B. A. Korgel; Chem. Mat., 2005, 17, 5705.
[13] Y. Ke, X. J. Weng, J. M. Redwing, C. M. Eichfeld, T. R. Swisher, S. E. Mohney,Y. M. Habib; Nano Lett., 2009, 9, 4494.
[14] C. Y. Wen, M. C. Reuter, J. Bruley, J. Tersoff, S. Kodambaka, E. A. Stach,F. M. Ross; Science, 2009, 326, 1247.
[15] T. E. Clark, P. Nimmatoori, K. K. Lew, L. Pan, J. M. Redwing,E. C. Dickey; Nano Lett., 2008, 8, 1246.
[16] S. T. He, S. S. Xie, J. N. Yao, H. J. Gao,S. J. Pang; Applied Physics Letters, 2002, 81, 150.
[17] C. Cavelius. Saarland University, 2009.
[18] F. A. Nichols; Journal of Applied Physics, 1966, 37, 2805.
[19] F. M. Davidson, D. C. Lee, III, D. D. Fanfair,B. A. Korgel; Journal of Physical Chemistry C, 2007, 111, 2929.
[20] K.-C. Chen, W.-W. Wu, C.-N. Liao, L.-J. Chen,K. N. Tu; Science, 2008, 321, 1066.
[21] M. Karimi, T. Tomkowski, G. Vidali,O. Biham; Physical Review B, 1995, 52, 5364.
[22] S. A. Morin,S. Jin; Nano Lett., 2010, 10, 3459.
[23] H. O. Pierson *Handbook of Chemical Vapor Deposition (CVD) - Principles, Technology and Applications (2nd Edition)*. 2nd Edition ed.; 1999.
[24] S. Hofmann, R. Sharma, C. T. Wirth, F. Cervantes-Sodi, C. Ducati, T. Kasama, R. E. Dunin-Borkowski, J. Drucker, P. Bennett,J. Robertson; Nature Materials, 2008, 7, 372.
[25] G. W. Sears; Acta Metallurgica, 1955, 3, 361.